

A Mach-Zehnder Interferometry Method for the Measurement of Photonic State Squeezing in Quantum Cavities

Siamak Khademi^{1, *}, Ghasem Naeimi^{1, 2}, and Ozra Heibati¹

Abstract—Recently, manipulation and measurement of quantum states, especially in quantum cavities, have attracted the attention of many researchers in different fields, such as quantum optics, quantum information, and quantum computation. In this paper, a non-demolition method for the measurement of squeezing parameter via atomic Mach-Zehnder interferometer is presented. An experimental setup was also proposed which included two quantum cavities, in different arms of an atomic Mach-Zehnder interferometer. Each quantum cavity was settled between two classical cavities. Quantum cavities contained entangled states with arbitrary squeezed photons. It is shown that the outgoing atomic states of Mach-Zehnder interferometer carry on the properties and situation of quantum states of the cavities. The squeezing parameter of photonic state for one of the cavities is obtained by the detection of excited and non-excited probabilities of Mach-Zehnder interferometer's outgoing ports, for a train of incoming two-level Rydberg atoms.

1. INTRODUCTION

The concepts and applications of nonclassical states like squeezing and entangled states have been considered by many authors [1–4]. Recently, squeezing and entangled states have found many applications in different fields [5–8], and many experimental setups have been presented to check the properties and applications of quantum entangled states [9–11]. Measurement and manipulation of quantum states, especially in quantum cavities, are a milestone for the development and improvement of atom-photon interaction methods [12–14], quantum teleportation [15], quantum cryptography [16], measuring the Wigner function of cavity field [17, 18], detecting photons in a cavity by non-demolition method [4, 19], quantum information and invention of quantum computers [20, 21], etc. A winner of the Nobel Prize, Serge Haroche, has presented an interesting non-demolition method for measuring Wigner function in a quantum cavity [12]. On the other hand, the Mach-Zehnder interferometry is applied to Bell's inequality [22, 23], electronic Mach-Zehnder interferometer (MZI) [24], single and two photon interferometry [25, 26], production and observation of Greenberger-Horne-Zeilinger entanglement [27], and optical amplification [28, 29].

In this article, another experimental setup is presented, which consists of an atomic MZI and a triplet array of cavities in each arm (see Figure 1). A train of individual excited Rydberg atoms was injected into the atomic MZI. Their atomic states were divided by the first atomic beam splitter and traveled in different MZI's arms, interacted with the cavity fields, and re-interfered by the second beam splitter. It was shown that the measurement of atomic states after the outgoing ports of the second beam splitter could simultaneously provide the amount of squeezing parameter of the photonic states, which are trapped in two different quantum cavities.

Received 15 January 2019, Accepted 15 April 2019, Scheduled 31 July 2019

* Corresponding author: Siamak Khademi (khademi@znu.ac.ir).

¹ Department of Physics, University of Zanjan, Zanjan, Iran. ² Physics Groups, Qazvin Branch, Islamic Azad University, Qazvin, Iran.

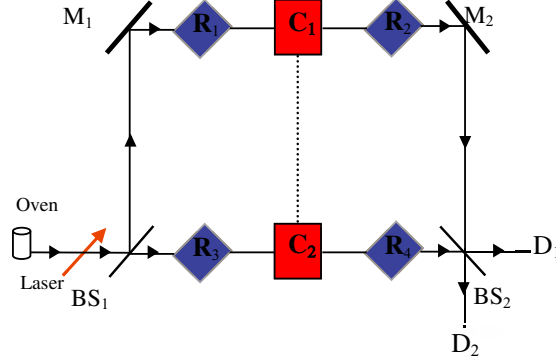


Figure 1. In a Mach-Zehnder interferometer, two arrays of triple cavities, including a quantum cavity (denoted by C, Red Square) between two classical cavities (denoted by R, Blue Diamond), are set in different paths. The photonic states in the quantum cavities are squeezed and entangled with each other (indicated by dotted line). A train of Rubidium atoms which are ejected from an oven is excited into higher levels, by a laser beam to prepare the Rydberg atoms. The state of atoms and their probabilities are detected by two ionized detectors D_1 and D_2 .

In the next section, a brief review of our proposed model and method is presented. In Section 3, the MZI outgoing probabilities of excited and non-excited atomic states are discussed. Sensitivities of probabilities to the interferometer's internal phase shift, squeezing and superposition parameters are also investigated. In Section 4, an analytical evaluation of superposition and squeezing parameter is presented, where $\Delta\varphi = \pi$. The final section is devoted to the conclusions.

2. MODEL AND METHOD: A BRIEF REVIEW

An interaction between a beam of Rydberg (e.g., Rubidium) atom and a cavity field has been theoretically and experimentally studied [12–14, 19, 30, 31]. The Rydberg atom whose valance electron is excited into higher atomic levels (e.g., the levels with the principal quantum number of 49, 50, or 51 labeled by as f , g , and e levels, respectively) is considered here. These atoms interact with both classical and quantized fields of cavities. In the present experimental setup, two arrays of quantum cavities, each including a quantum cavity C between two classical cavities R 's, were settled in two arms of atomic MZI, as depicted in Fig. 1. The quantum cavities C_j ($j = 1, 2$) were tuned to have a non-resonance interaction ($\delta = \omega_f - \omega_a \neq 0$) between the trapped photons, with frequency of ω_f , and two atomic levels of e and g , with the transition frequency of ω_a . The electromagnetic field within the classical cavities R_k ($k = 1$ and 2 for the clockwise (CW) and 3 and 4 for the counter clockwise (CCW) arms) interacted resonantly ($\delta = \omega_f - \omega_a = 0$) with the transition frequency of f and g atomic levels. Thus, in each cavity, there was a two-level atom interaction with the electromagnetic fields.

In a semi-classical model of a two-level atom and electromagnetic field interaction, the populations of atomic states oscillate with the Rabi frequency Ω_R [30, 31]. A full-quantum model of a two-level atom and quantized electromagnetic field interaction has also been described by Jaynes-Cummings model [30, 31].

For the classical cavities R_s interaction Hamiltonian for a two-level atom and classic electromagnetic field is given by $H_{sc}(t) = \hat{V}_0 \cos \omega_f t$, where $\hat{V}_0 = -\hat{\mathbf{d}} \cdot \mathbf{E}_0$, and $\hat{\mathbf{d}}$ and \mathbf{E}_0 are the electric dipolar moment of atom and the electric field amplitude, respectively. Consider the electromagnetic field in the classical cavity R is tuned to interact with f and g levels of atomic state, where the atoms are initially in the $|g\rangle$ state. The atomic state after interaction is evolved as:

$$|\psi(t)\rangle = e^{-i\hat{H}(t)/\hbar} |g\rangle = \cos\left(\frac{\Omega_R t}{2}\right) |g\rangle + i \sin\left(\frac{\Omega_R t}{2}\right) |f\rangle, \quad (1)$$

where $\Omega_R = \nu/\hbar$ is the classical Rabi frequency and $\nu = \langle g | \hat{V}_0 | f \rangle = -\hat{\mathbf{d}}_{gf} \cdot \mathbf{E}_0$. If the atoms are initially

in state $|f\rangle$, the final state after interaction is evolved as:

$$|\psi(t)\rangle = e^{-i\hat{H}^{(I)}t/\hbar} |f\rangle = \cos\left(\frac{\Omega_R t}{2}\right) |f\rangle + i \sin\left(\frac{\Omega_R t}{2}\right) |g\rangle. \quad (2)$$

The flight time t is the traveling time of atom through the electromagnetic field in the cavity.

For the quantum cavity C , Jaynes-Cummings Hamiltonian $\hat{H}_{JC} = \hbar\lambda(\hat{\sigma}_+\hat{a} + \hat{\sigma}_-\hat{a}^\dagger)$ [30, 31] describes the interaction between the quantized electromagnetic field $\hat{\mathbf{E}} = \mathbf{e}(\hbar\omega/\varepsilon_0 V)^{1/2}(\hat{a} + \hat{a}^\dagger)\sin(kz)$ and two-level Rydberg atoms, where $\hat{a}^\dagger(\hat{a})$ is the creation (annihilation) operator, $\lambda = -\frac{d}{\hbar}(\hbar\omega/\varepsilon_0 V)^{1/2}\sin kz$, and $\hat{\sigma}_\pm$ are the transition operators between the atomic levels e and g (where $\hat{\sigma}_+ = |e\rangle\langle g| = \hat{\sigma}_-^\dagger$). In a non-resonant interaction regime and a few calculations, the Jaynes-Cummings Hamiltonian is transformed into $\hat{H}_{eff} = \hbar\chi(\hat{\sigma}_+\hat{\sigma}_- + \hat{a}^\dagger\hat{a}\hat{\sigma}_3)$, where $\chi = \lambda^2/\delta$. If the initial state of the atom field is given as $|\psi(t=0)\rangle = |e\rangle|n\rangle$ or $|\psi(t=0)\rangle = |g\rangle|n\rangle$, the final state is obtained as:

$$|\psi(t)\rangle = e^{-i\hat{H}_{eff}t/\hbar} |e\rangle|n\rangle = e^{-i\chi(n+1)t} |e\rangle|n\rangle, \quad (3)$$

or

$$|\psi(t)\rangle = e^{-i\hat{H}_{eff}t/\hbar} |g\rangle|n\rangle = e^{i\chi n t} |g\rangle|n\rangle, \quad (4)$$

respectively. In these cases, the states of atom-field just have a phase which is proportional to the number of photons; therefore, the atoms have no transition between the atomic levels during this interaction. If the photonic state of quantum cavity is a squeezed number state, the final states also depend on the squeezing parameter as:

$$|e\rangle|n, r\rangle \rightarrow e^{-i\hat{H}_{eff}(r)t/\hbar} |e\rangle|n, r\rangle \rightarrow e^{-i\chi((2n+1)\cosh^2 r - n)t} |e\rangle|n, r\rangle, \quad (5)$$

$$|g\rangle|n, r\rangle \rightarrow e^{-i\hat{H}_{eff}(r)t/\hbar} |g\rangle|n, r\rangle \rightarrow e^{i\chi((2n+1)\cosh^2 r - (n+1))t} |g\rangle|n, r\rangle \quad (6)$$

$$|f\rangle|n, r\rangle \rightarrow e^{-i\hat{H}_{eff}(r)t/\hbar} |f\rangle|n, r\rangle \rightarrow |f\rangle|n, r\rangle, \quad (7)$$

where the effective interaction Hamiltonian for atom and squeezed photons is obtained from:

$$\hat{H}_{eff}(r) = \hbar\chi[\hat{\sigma}_+\hat{\sigma}_- + (S^{-1}(r)\hat{a}^\dagger S(r))(S^{-1}(r)\hat{a} S(r))\hat{\sigma}_3]. \quad (8)$$

In relations (5)–(7), the squeezed state of number state of the photons is given by:

$$|n, \xi\rangle = \hat{S}(\xi)|n\rangle. \quad (9)$$

The unitary squeezed operator is defined as $\hat{S}(\xi) = \exp\left(\frac{1}{2}\xi^* \hat{a}^2 - \frac{1}{2}\xi \hat{a}^{\dagger 2}\right)$ where $\xi = re^{i\theta}$. Parameters r and θ are the squeezing parameter and squeezing phase [30, 31], respectively. For relations (5)–(8) and hereafter, the squeezing phase is assumed to be zero for simplicity.

3. MZI OUTGOING PROBABILITIES

In the proposed experimental setup, the states of quantum cavities C_1 and C_2 are initially prepared to be entangled as:

$$|\psi\rangle = \alpha|0, r\rangle_1|1\rangle_2 + \sqrt{(1-|\alpha|^2)}|1, r\rangle_1|0\rangle_2. \quad (10)$$

Different values of α provide different amounts of entanglement, and its maximum entanglement is given by $\alpha = 0.5$. In relation (10), state of the photons in the quantum cavity C_1 is assumed to be squeezed with an unknown squeezing parameter r , while (for simplicity) the second quantum cavity C_2 is not. A scheme of the proposed experimental setup which includes an MZI is depicted in Fig. 1, where beam splitters are illustrated by BS_1 and BS_2 , and mirrors are indicated by M_1 and M_2 . A train of individual Rubidium atoms is produced, and their states are transformed into Rydberg atoms initially in the state $|g\rangle$ by a laser pump before BS_1 . Each atom is passed through the MZI, independent of the previous and next one. The incoming atomic states are divided by a symmetric 50–50 BS_1 , passing through the CW or CCW arms of MZI, and recombined (or interfere again) by another symmetric 50–50 BS_2 . The states of outgoing atoms are measured by detectors D_1 and D_2 . The dotted line between quantum

cavities in Fig. 1 indicates their entanglement. In each arm of MZI, there is a triplet cavity consisting of two classical cavities on the sides and one quantum cavity in the middle. The classical (quantum) cavities and their electromagnetic fields are set to interact with the atoms resonantly (non-resonantly). Quantum cavities interact with $|g\rangle$ and $|e\rangle$ atomic states with phase π , have a high Q-factor, and are made of an open Fabry-Perot resonator with two superconducting Niobium spherical mirrors. The R_i 's ($i = 1, 2, 3, 4$) cavities contain classical electromagnetic fields which resonantly interact with $|g\rangle$ and $|e\rangle$ atomic states. The atoms interact with classical cavities, where the phases of R_1 , R_2 , and R_3 are $\Omega_R t = \pi/2$, and the phase in R_4 is $\Omega_R t = 3\pi/2$.

The BS₁ divided incoming state $|g\rangle$ into $|\psi'\rangle_1 = |g\rangle/\sqrt{2}$ and $|\psi'\rangle_2 = |g\rangle/\sqrt{2}$ in the CW and CCW arms, respectively:

$$\begin{pmatrix} |\psi'\rangle_1 \\ |\psi'\rangle_2 \end{pmatrix} = \frac{1}{\sqrt{2}} \begin{pmatrix} 1 & 1 \\ 1 & -1 \end{pmatrix} \begin{pmatrix} |g\rangle \\ 0 \end{pmatrix}, \quad (11)$$

where $\frac{1}{\sqrt{2}} \begin{pmatrix} 1 & 1 \\ 1 & -1 \end{pmatrix}$ is the beam splitter operator. In the CW arm, the atom passes through the upper cavities array, as illustrated in Fig. 1. After passing through cavity R_1 , the atomic states are transformed into a superposition state $(|g\rangle + i|f\rangle)/\sqrt{2}$. The total CW atom-field state is obtained as:

$$\begin{aligned} |Atom - Field\rangle_{CW} &= |\psi'\rangle_1 (\alpha|o, r\rangle_1|1\rangle_2 + \beta|1, r\rangle_1|0\rangle_2) \\ &\xrightarrow{R_1, \pi/2} \frac{1}{\sqrt{2}} \left[\frac{1}{\sqrt{2}}(|g\rangle + i|f\rangle) \right] (\alpha|o, r\rangle_1|1\rangle_2 + \beta|1, r\rangle_1|0\rangle_2). \end{aligned} \quad (12)$$

Relations (2) and (3) are used to derive Eq. (12) where $\beta = \sqrt{1 - |\alpha|^2}$ and $\Omega_R t = \pi/2$. Relations (6), (7), and (12) with the interaction phase π are applied to obtain the effect of quantum cavity C_1 (with squeezed field) on its incoming state (12) as:

$$\begin{aligned} |Atom - Field\rangle_{CW} &\xrightarrow{C_1, \pi} \frac{1}{2} [|g\rangle (-\alpha e^{i\gamma \cosh^2 r} |0, r\rangle_1 |1\rangle_2 \\ &\quad + \beta e^{i3\pi \cosh^2 r} |1, r\rangle_1 |0\rangle_2) + i|f\rangle (\alpha |0, r\rangle_1 |1\rangle_2 + \beta |1, r\rangle_1 |0\rangle_2)]. \end{aligned} \quad (13)$$

Relation (13) shows that the quantized electromagnetic fields in quantum cavities are entangled with the atom, where the atom passes through the cavity R_2 with interaction phase $\Omega_R t = \pi/2$. The atomic states $|g\rangle$ and $|f\rangle$ in Eq. (13) are transformed into states $(|g\rangle + i|f\rangle)/\sqrt{2}$ and $(|f\rangle + i|g\rangle)/\sqrt{2}$, respectively. The CW atom-field state that enters the port of the second beam splitter BS₂ is obtained as:

$$\begin{aligned} |Atom - Field\rangle_{CW} &= \frac{1}{2\sqrt{2}} [|g\rangle (-\alpha (1 + e^{i\gamma}) |0, r\rangle_1 |1\rangle_2 - \beta (1 - e^{i3\gamma}) |1, r\rangle_1 |0\rangle_2) \\ &\quad + i|f\rangle (\alpha (1 - e^{i\gamma}) |0, r\rangle_1 |1\rangle_2 + \beta (1 + e^{i3\gamma}) |1, r\rangle_1 |0\rangle_2)] e^{i\varphi_1}. \end{aligned} \quad (14)$$

where $\gamma = \pi \cosh^2 r$ is a function of squeezing parameter, and the total phase shift due to the path length and mirrors reflections is shown by $e^{i\varphi_1}$.

In the CCW path, the atomic states were transformed by passing through the second array of cavities, in which the interaction phases for the cavities R_3 , C_2 , and R_4 are $\pi/2$, π , $3\pi/2$, respectively. So, the total interferometer's internal phase shift due to the path length and mirror reflections is given by $e^{i\varphi_2}$.

The atom-field state in the CCW arm that enters the next port of the second beam splitter is obtained similarly as:

$$|Atom - Field\rangle_{CCW} = \frac{1}{2\sqrt{2}} [-2i\alpha |f\rangle |0, r\rangle_1 |1\rangle_2 - 2\beta |g\rangle |0, r\rangle_1 |0\rangle_2] e^{i\varphi_2}. \quad (15)$$

The CW and CCW states in Eqs. (14) and (15) are recombined by the second beam splitter BS₂, and outgoing states are obtained by applying the beam splitter operator on the incoming states:

$$\begin{pmatrix} |Out\rangle_1 \\ |Out\rangle_2 \end{pmatrix} = \frac{1}{\sqrt{2}} \begin{pmatrix} 1 & 1 \\ 1 & -1 \end{pmatrix} \begin{pmatrix} |Atom - Field\rangle_{CW} \\ |Atom - Field\rangle_{CCW} \end{pmatrix}, \quad (16)$$

The detectors D_1 and D_2 measure the state of outgoing atomic states from two ports of BS₂ and are indicated by indices 1 and 2, respectively. Therefore, they measure four outgoing probabilities P_{gD_1} , P_{fD_1} , P_{gD_2} , and P_{fD_2} , where P_{iD_j} is the probability of finding the atoms in the i th state by the j -th detector. These probabilities are obtained from relations (14)–(16) as:

$$P_{gD_1} = (1 + \alpha^2 \cos(\gamma) + \beta^2(2 - \cos(3\gamma) - 2\cos(\Delta\varphi + 3\gamma) + 2\cos(\Delta\varphi)))/8, \quad (17)$$

$$P_{fD_1} = (1 + \alpha^2(2 + 2\cos(\Delta\varphi + \gamma) - \cos(\gamma) - 2\cos(\Delta\varphi)) + \beta^2 \cos(3\gamma))/8, \quad (18)$$

$$P_{gD_2} = (1 + \alpha^2 \cos(\gamma) + \beta^2(2 - \cos(3\gamma) + 2\cos(\Delta\varphi + 3\gamma) - 2\cos(\Delta\varphi)))/8, \quad (19)$$

$$P_{fD_2} = (1 + \alpha^2(2 - 2\cos(\Delta\varphi + \gamma) - \cos(\gamma) + 2\cos(\Delta\varphi)) + \beta^2 \cos(3\gamma))/8, \quad (20)$$

where $\Delta\varphi = \varphi_1 - \varphi_2$ is the total internal phase difference between the two arms of MZI. Clearly, these probabilities are sensitive to the squeezing parameter r , superposition coefficient α , and internal phase difference $\Delta\varphi$. Therefore, the MZI in our proposed experimental setup is a suitable instrument for the measurements of squeezing and superposition parameters.

Figures 2(a)–2(d) show the probabilities of atomic states in Eqs. (17)–(20) in terms of internal phase difference $\Delta\varphi$, detection by two ionized detectors for $\alpha = 0$, and different values of small squeezing parameter $r = \{0, .1, .2, .3, .4, .5\}$. The probabilities P_{gD_1} and P_{gD_2} have a periodic behavior. Their

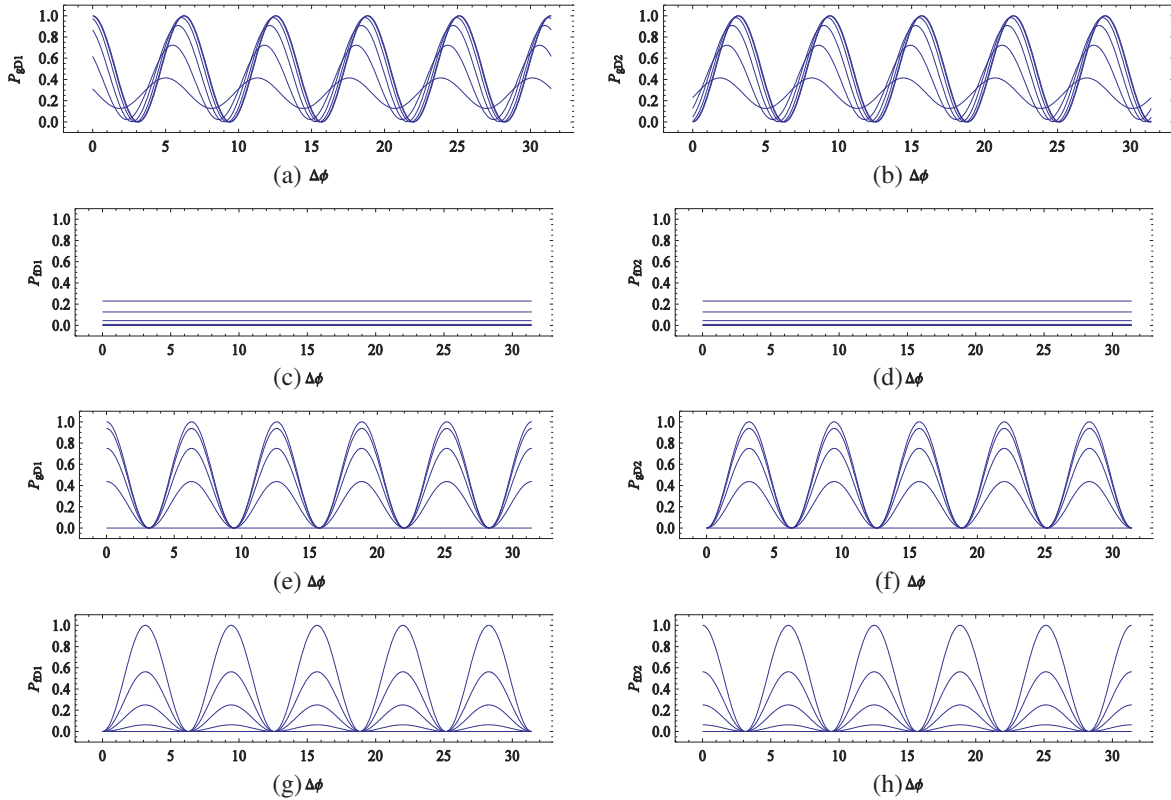


Figure 2. (a)–(d) Probabilities of atomic states outgoing of MZI in terms of internal path phase shift, detected by two ionized detectors for $\alpha = 0$ and $r = \{0, .1, .2, .3, .4, .5\}$. (a) and (b) have a periodic behaviour for probabilities P_{gD_1} and P_{gD_2} , respectively. The maximum of probabilities are decreased and also have a phase shift by increasing the squeezing parameter. (c) and (d) probabilities P_{fD_1} and P_{fD_2} are constant and are increased by increasing the squeezing parameter. (e)–(h) the probabilities are plotted for $r = 0$ and $\alpha = \{0, .25, .5, .75, 1\}$. All have a periodic behavior in terms of internal phase difference. (e) and (f) maximum probabilities of detecting g-state are decreased by increasing the superposition coefficient α . (g) and (h) maximum probabilities of f-state detection are increased by increasing the superposition coefficient α . In all plots, the squeezing parameters are supposed to be small.

peaks are decreased and suffer a phase shift by increasing the (small) squeezing parameter. The probabilities P_{fD_1} and P_{fD_2} are also constant for all the phase shifts $\Delta\varphi$. Figures 2(e)–2(h) represent the corresponding probabilities for $\alpha = (0, .25, .5, .75, 1)$, where the squeezing parameter is vanishing. All the probabilities have a periodic behavior in terms of $\Delta\varphi$. The peaks of probabilities P_{gD_1} and P_{gD_2} are decreased (P_{fD_1} and P_{fD_2} are increased) by increasing the superposition coefficient α .

Larger squeezing parameters are also investigated. Figures 3(a)–3(d) demonstrate that all probabilities at a constant internal phase difference (e.g., $\Delta\varphi = 0$) have an oscillatory behavior in terms of squeezing parameter r . Their periods are decreased by increasing the squeezing parameter. Figures 2 and 3 show that the probabilities are sensitive to the amounts of squeezing and superposition coefficients.

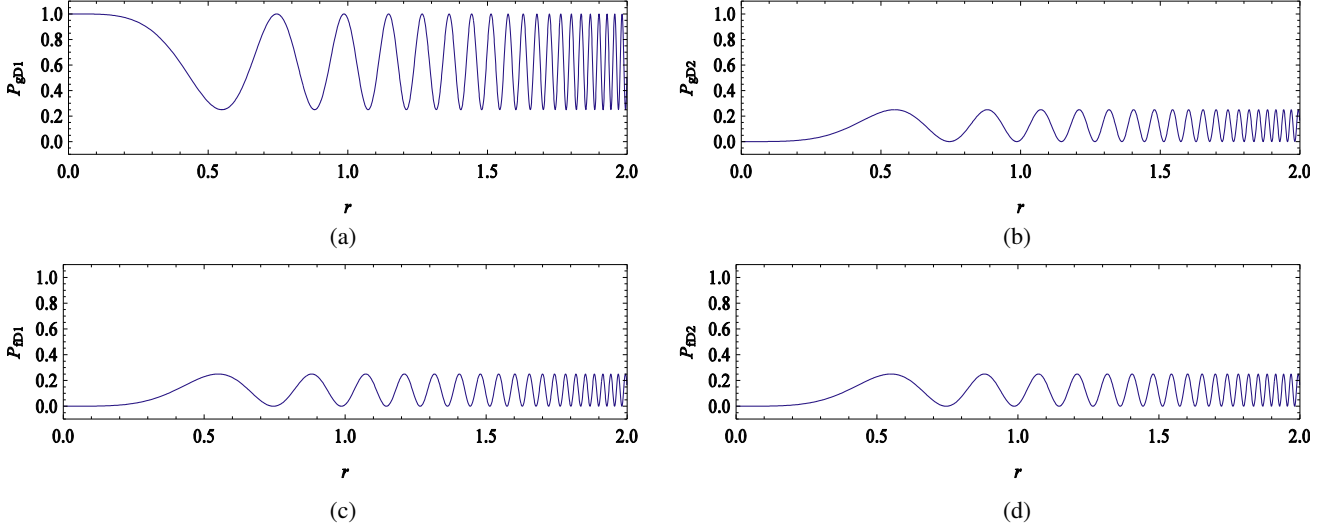


Figure 3. All probabilities have an oscillatory behavior with a decreasing period for larger squeezing parameters. In this case, the internal phase difference and superposition coefficient are supposed to be $\Delta\varphi = 0$ and $\alpha = 0$.

Also, probabilities (17)–(20), as well as $C_1 = P_{gD_1} - P_{gD_2}$ and $C_2 = P_{fD_1} - P_{fD_2}$, give us a numerical solution of C_1 and C_2 in terms of $\Delta\varphi$ and α where the squeezing parameter vanishes, $r = 0$. The difference probabilities C_1 and C_2 are plotted in terms of $\Delta\varphi$ and α , in Figure 4. Clearly, C_1 (C_2) is more sensitive to internal phase difference $\Delta\varphi$ for small (large) values of superposition parameter.

4. SQUEEZING AND SUPERPOSITION PARAMETERS

Outgoing probabilities are useful, and in general sufficient, to evaluate squeezing and superposition parameters for the photonic states of the corresponding quantum cavities. For practical purposes, the internal phase difference is controllable by a simple phase shifter. Therefore, without any loss of generality, the internal phase difference is supposed to be $\Delta\varphi = \pi$. Then, the squeezing r or equivalently $\gamma = \pi \cosh^2 r$ and the superposition parameter α can be analytically obtained. In this case, the probabilities are obtained as:

$$P_{gD_1} = P_{fD_2} = \frac{1}{8} (1 + \alpha^2 \cos(\gamma) + (1 - \alpha^2) \cos(3\gamma)), \quad (21)$$

$$P_{fD_1} = \frac{1}{8} (1 + \alpha^2(4 - 3 \cos(\gamma)) + (1 - \alpha^2) \cos(3\gamma)), \quad (22)$$

$$P_{gD_2} = \frac{1}{8} (1 + \alpha^2 \cos(\gamma) + (1 - \alpha^2)(4 - 3 \cos(3\gamma))). \quad (23)$$

Using relations (21)–(23) and the identity $\cos(3u) = 3 \cos^2(u) \sin(u) - \sin^3(u)$ to neglect $\cos(\gamma)$ and some straightforward calculations to find: $C_1 = C_2(3 + 4C_2/\alpha^2)^2(-1 + \alpha^2)/\alpha^2$ and $\cos^2(\gamma/2) = 1 + C_2/\alpha^2$.

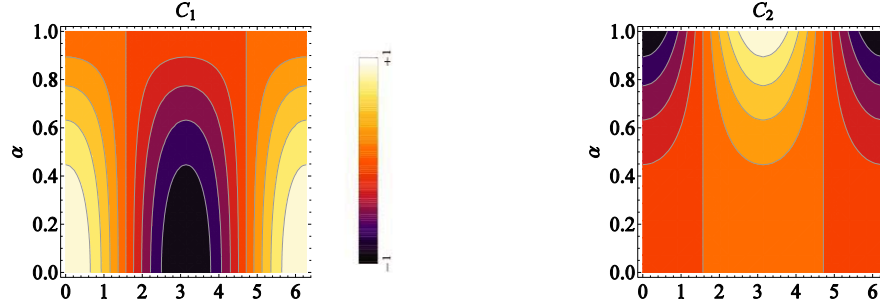


Figure 4. The probability differences are plotted in terms of superposition parameter (vertical axis) and interferometer's internal phase shift (horizontal axis), where the squeezing parameter $r = 0$.

The superposition parameters α and $\cos(\gamma/2)$ are obtained analytically as:

$$\alpha^2 = \frac{(S_0 + 9C_2S_1 - 24C_2^2S_1 + 3^{1/3}S_1^2)}{(3S_1(C_1 + 9C_2))}, \quad (24)$$

and

$$\cos(\gamma/2) = \frac{2C_2(3S_1(C_1 + 9C_2))}{(S_0 + 9C_2S_1 - 24C_2^2S_1 + 3^{1/3}S_1^2)} + 1, \quad (25)$$

where

$$S_1 = 8\sqrt{3}\sqrt{C_1C_2^6(C_1 + 9C_2)^2(27C_1 + (3 + 4C_2)^3)} + 9C_2^3(8C_1^2 + (3 + 4C_2)^3 + 4C_1(9 + 2C_2(3 + 8C_2)))^{1/3} \quad (26)$$

and

$$S_0 = 3^{2/3}C_2^2(8C_1(3 - 2C_2) + 3(3 + 4C_2)^2). \quad (27)$$

Equations (24) and (25) give us an analytical calculation of squeezing and superposition parameters where the internal phase difference of MZI is set to π . Our method does not destruct the quantum states of cavities, hence it is a non-demolition measurement method.

5. CONCLUSIONS

In this paper, an experimental method is proposed to measure the squeezing and superposition parameters of photonic states for two quantum cavities settled in an MZI. The MZI has a set of triple cavities in each arm. Each triple cavity has a quantum cavity in each arm in the middle of two classical cavities. The squeezed states of photons in the quantum cavities are set to be entangled. In the present method, the atomic states in the outgoing ports of the MZI and also their probabilities' detection depend on the amount of internal phase difference, superposition coefficient, and squeezing parameters of photonic states in quantum cavities. The behaviors of outgoing probabilities are studied in terms of squeezing parameter or superposition coefficient, in special cases. It is shown that measurements of outgoing ports probabilities provide the squeezing parameter and superposition coefficient simultaneously for a special internal phase difference, either numerically or analytically.

The peaks curves in Figures (2a)–(2b) and values of curves in Figures (2c)–(2d) depend on the squeezing parameter. When $\alpha = 0$ and $r = \{0, .1, .2, .3, .4, .5\}$, the probabilities P_{gD1} and P_{gD2} have a periodic behaviour whose peaks are decreased and also have a phase shift by increasing the squeezing parameter. In Figures (2c)–(2d), the probabilities P_{fD1} and P_{fD2} are constant and are increased by increasing the squeezing parameter. Both of coupled probabilities $\{P_{gD1}, P_{gD2}\}$ or $\{P_{fD1}, P_{fD2}\}$ are suitable for the measurement of squeezing parameter r independently.

Also, the outgoing probabilities, Figures (2e)–(2h), are plotted for $r = 0$ and $\alpha = (0, .25, .5, .75, 1)$. All curves have a periodic behavior in terms of internal phase difference. The maximum probabilities of P_{gD1} and P_{gD2} (P_{fD1} and P_{fD2}) are decreased (increased) by increasing the superposition coefficient α .

REFERENCES

1. Einstein, B. Podolsky, and N. Rosen, "Can quantum-mechanical description of physical reality be considered complete?" *Phys. Rev.*, Vol. 47, 777, 1935.
2. Bohr, N., "Can quantum-mechanical description of physical reality be considered complete?," *Phys. Rev.*, Vol. 48, 696–702, 1935.
3. Sadeghi, P., S. Khademi, and S. Nasiri, "Nonclassicality indicator for the real phase-space distribution function," *Phys. Rev. A*, Vol. 82, 012102, 2010.
4. Naeimi, G., S. Alipour, and S. Khademi, "A photon counting and a squeezing measurement method by the exact absorption and dispersion spectrum of Λ -type atoms," *Springer Plus*, Vol. 5, 1402, 2016.
5. He, X. L., Q. P. Su, F. Y. Zhang, and C. P. Yang, "Generating multipartite entangled states of qubits distributed in different cavities," *Quantum Information Processing*, Vol. 13, 1381–1395, 2014.
6. Shahidani, S., M. H. Naderi, M. Soltanolkotabi, and S. Barzanjeh, "Steady-state entanglement, cooling, and tristability in a nonlinear optomechanical cavity," *JOSA B*, Vol. 31, 1087–1095, 2014.
7. Khademi, S., G. Naeimi, and O. Heibati, "A simple scheme for generation of N-qubits entangled states," *Applied Mathematics and Physics*, Vol. 2, 1–3, 2014.
8. Xiong, W. and L. Ye, "Schemes for entanglement concentration of two unknown partially entangled states with cross-Kerr nonlinearity," *JOSA B*, Vol. 28, 2030–2037, 2011.
9. Wolters, J., J. Kabuss, A. Knorr, and O. Benson, "Deterministic and robust entanglement of nitrogen-vacancy centers using low- Q photonic-crystal cavities," *Phys. Rev. A*, Vol. 89, 060303(R), 2014.
10. Kaiser, F., L. A. Ngah, A. Issautier, T. Delord, D. Aktas, V. DAuria, M. P. De Micheli, A. Kastberg, L. Labonté, O. Alibert, A. Martin, and S. Tanzilli, "Polarization entangled photon-pair source based on quantum nonlinear photonics and interferometry," *Optics Communications*, Vol. 327, 7–16, Special Issue on Nonlinear Quantum Photonics, 2014.
11. Schliemann, J., "Entanglement thermodynamics," *J. Stat. Mech.*, P09011, 2014.
12. Brune, M., S. Haroche, J. M. Raimond, L. Davidovich, and N. Zagury, "Manipulation of photons in a cavity by dispersive atom-field coupling: Quantum-nondemolition measurements and generation of "Schrödinger cat" states," *Phys. Rev. A*, Vol. 45, 5193, 1992.
13. Raimond, J. M., M. Brune, and S. Haroche, "Manipulating quantum entanglement with atoms and photons in a cavity," *Rev. Mod. Phys.*, Vol. 73, 565, 2001.
14. Khademi, S. and S. Alipour, "A non-demolition photon counting method by four-level inverted Y-type atom," *International Journal of Optics and Photonics*, Vol. 11, 63–74, 2017.
15. Bussieres, F., C. Clausen, A. Tiranov, B. Korzh, V. B. Verma, S. W. Nam, F. Marsili, A. Ferrier, P. Goldner, H. Herrmann, C. Silberhorn, W. Sohler, M. Afzelius, and N. Gisin, "Quantum teleportation from a telecom-wavelength photon to a solid-state quantum memory," *Nature Photonics*, Vol. 8, 775–778, 2014.
16. Luda, M. A., M. A. Larotonda, J. P. Paz, and C. T. Schmiegelow, "Manipulating transverse modes of photons for quantum cryptography," *Phys. Rev. A*, Vol. 89, 042325, 2014.
17. Sridhar, N., R. Shahrokhshahi, A. J. Miller, B. Calkins, T. Gerrits, A. Lita, S. W. Nam, and O. Pfister, "Direct measurement of the Wigner function by photon-number-resolving detection," *JOSA B*, Vol. 31, B34–B40, 2014.
18. Banaszek, K., C. Radzewicz, K. Wodkiewicz, and J. S. Krasinski, "Direct measurement of the Wigner function by photon counting," *Phys. Rev. A*, Vol. 60, 674–677, 1999.
19. Naeimi, G., S. Khademi, and O. Heibati, "A method for the measurement of photons number and squeezing parameter in a quantum cavity," *ISRN Optics*, 271951, 2013.
20. Zheng, S. B., "Quantum-information processing and multiatom-entanglement engineering with a thermal cavity," *Phys. Rev. A*, Vol. 66, 060303(R), 2002.

21. Li, W. and I. Lesanovsky, "Entangling quantum gate in trapped ions via Rydberg blockade," *Applied Physics B*, Vol. 114, 37–44, 2014.
22. Johansen, L. M., "Bell's inequality for the Mach-Zehnder interferometer," *Phys. Lett. A*, Vol. 219, 15–18, 1996.
23. Kang, K. and K. H. Lee, "Violation of Bell's inequality in electronic Mach-Zehnder interferometers," *Physica E: Low-dimensional Systems and Nanostructures*, Vol. 40, 1395–1397, 2008.
24. Ji, Y., Y. Chung, D. Sprinzak, M. Heiblum, D. Mahalu, and H. Shtrikman, "An electronic Mach-Zehnder interferometer," *Nature*, Vol. 422, 415–418, 2003.
25. Seigneur, H. P., M. N. Leuenberger, and W. V. Schoenfeld, "Single-photon Mach-Zehnder interferometer for quantum networks based on the single-photon Faraday effect," *J. Appl. Phys.*, Vol. 104, 014307, 2008.
26. Carlos Ryff, L. and P. H. Souto Ribeiro, "Mach-Zehnder interferometer for a two-photon wave packet," *Phys. Rev. A*, Vol. 63, 023801, 2001.
27. Vyshnevyy, A. A., G. B. Lesovik, T. Jonckheere, and T. Martin, "Setup of three Mach-Zehnder interferometers for production and observation of Greenberger-Horne-Zeilinger entanglement of electrons," *Phys. Rev. B*, Vol. 87, 165417, 2013.
28. Nady Abdul Aleem, M., K. F. A. Hussein, and A.-E.-H. A.-E.-A. Ammar, "Ultrafast all-optical full adder using quantum-dot semiconductor optical amplifier-based Mach-Zehnder interferometer," *Progress In Electromagnetics Research B*, Vol. 54, 69–88, 2013.
29. Dimitriadou, E. and K. E. Zoiros, "On the feasibility of 320 GB/S all-optical and gate using quantum-dot semiconductor optical amplifier-based Mach-Zehnder interferometer," *Progress In Electromagnetics Research B*, Vol. 50, 113–140, 2013.
30. Gerry, C. and P. Knight, *Introductory Quantum Optics*, University Press, Cambridge, 2004.
31. Scully, M. O. and M. S. Zubairy, *Quantum Optics*, University Press, Cambridge, 1997.